

Assistance using adaptive oscillators: Sensitivity analysis on the resonance frequency

Mike Domenik Rinderknecht*, Fabien André Delaloye*, Alessandro Crespi*,
Renaud Ronsse*[†], and Auke Jan Ijspeert*

* Biorobotics Laboratory; Institute of Bioengineering

École Polytechnique Fédérale de Lausanne (EPFL), CH-1015 Lausanne, Switzerland

Email: {mikedomenik.rinderknecht,fabien.delaloye,alessandro.crespi,auke.ijspeert}@epfl.ch

[†] Centre for Research in Mechatronics; Institute of Mechanics, Materials, and Civil Engineering

Université catholique de Louvain, B-1348 Louvain-la-Neuve, Belgium

Email: renaud.ronsse@uclouvain.be

Abstract—This paper provides a robustness analysis of the method we recently developed for rhythmic movement assistance using adaptive oscillators. An adaptive oscillator is a mathematical tool capable of extracting high-level features (i.e. amplitude, frequency, offset) of a quasi-sinusoidal measured movement, a rhythmic flexion-extension of the elbow in this case. By the use of a simple inverse dynamical model, the system can predict the torque produced by a human participant, such that a fraction of this estimated torque is fed back through a series elastic actuator to provide movement assistance. This paper objectives are twofold. First, we introduce a new 1 DOF assistive device developed in our lab. Second, we derive model-based predictions and conduct experimental validations to measure the variations in movement frequency as a function of the open parameters of the inverse dynamical model. As such, the paper provides an estimation of the robustness of our method due to model approximations. As main result, the paper reveals that the movement frequency is particularly robust to errors in the estimation of the damping coefficient. This is of high interest for the applicability of our approach, this parameter being in general the most difficult to quantify.

I. INTRODUCTION

Modern challenges in robotics research deal with applications involving close interactions between robots and humans [1]. This is particularly true in rehabilitation robotics, since the robots are in direct contact with the user’s effectors to assist movements. In particular, lower-limb rehabilitation or assistive exoskeletons have a structure which often goes in parallel to the user’s legs [2], [3].

All the exoskeletons need to face the critical issue of the human-robot interface [4] to optimize the robot behavior in movement assistance. Historically, the interface was unidirectional, the robot forcing the user’s legs to follow pre-defined trajectories using stiff position control [5], [6]. This approach had however some obvious limitations, the user being moved along the same trajectory whatever his/her own participation. Consequently, more recent approaches focused on collaborative, “assist-as-needed”, strategies [7], requiring compliance between the robot and the user. This can be achieved either through hardware adaptations [8], or by lowering the controller gains [9].

Another type of human-robot interface, which appeared

more recently, is also unidirectional, yet in the other direction. In this case, the user is supposed to fully control the robot in order to have it synchronized with his/her movement intentions. The robot should therefore detect the user motion intention (e.g. direction, velocity, amplitude) and react timely to provide the specific assistance needed by the user in terms of direction and absolute value. One way of realizing this kind of interface is by using surface EMG to provide the wearer with a fraction of the estimated desired torque [10], [11]. These approaches therefore implement a sort of torque amplifier. However, EMG-based approaches have some drawbacks, mainly related to signal acquisition, user-specific calibration, and poor accuracy in model-based torque estimation.

Recently, we introduced a new method for movement assistance which combines the advantages of both approaches [12], [13]. First, it assists the user during the execution of a quasi-sinusoidal movement by providing a fraction of the estimated torque. The user is free to modulate the parameters of the effector trajectory (amplitude, frequency, etc.), and the assistive device flexibly adapts. Second, it requires no complex sensing like surface EMG, since the sole variable that needs to be measured is the position of the assisted joint(s), obtained via a simple encoder.

The central block of this method is an adaptive oscillator [14], [15], which synchronizes with the joint movement and estimates its higher order derivatives. The intended torque is retrieved from an inverse model, and a fraction of it is fed back to the user, providing assistance. This method was first validated on a simple one degree-of-freedom (DOF) upper-limb movement [12], [13]. The extension of this method to a walking task (thus involving several DOFs) is a topic of on-going research and will be addressed in a separate paper.

The goals of the present paper are twofold. First, we present a new assistive device for the elbow which was designed in our lab, and which can be viewed as a simplified version of the exoskeleton used in [12], [13], [16]. Second, again on this single DOF task, we carried out a sensitivity analysis on the open parameters of the inverse model, in order to establish the robustness of our method on model approximations.

This analysis relies on the assumption that cyclical forearm

movements about the elbow and around the vertical equilibrium tend to be performed at the resonance frequency, i.e. the frequency minimizing the performer's effort by optimizing transfers between potential and kinetic energy [17]. Many results in the literature tend to illustrate that human cyclical movements are executed at the resonance frequency (see e.g. [18], [19], [20]). Therefore, we carried out a model-based study. First, the resonance frequency of the coupled system comprising the human elbow+forearm and the controlled assistive device was derived, both assuming a "correct" inverse model, and by purposely introducing errors in the estimates of the model parameters (such as mass, inertia, friction). Second, the movement frequency of human participants performing elbow movements while being assisted with the simulated models was measured, and compared to the predicted values. Finally, a sensitivity analysis was performed to see if the changes in movement frequency obey the trends as predicted by the model, and to what extent our method is robust to poor estimates of the model parameters.

II. METHODS

A. Kinematics estimation using adaptive oscillators

Assistance was provided using an adaptive oscillator, a tool developed by Righetti et al. [14], [15] and used in many applications [13], [21]. We used a simplified version of the modified Hopf oscillator proposed in [14], by projecting this oscillator into polar coordinates and keeping the phase equation only. We simply obtained an augmented phase oscillator [15]:

$$\dot{\phi}(t) = \omega(t) + \nu F(t) \cos \phi(t), \quad (1)$$

where $\omega(t)$ is the intrinsic frequency of the oscillator, and ν the learning parameter determining the speed of phase synchronization to the periodic input signal $F(t)$. In order to learn the frequency of the input $F(t)$, instead of doing mere synchronization only, the oscillator frequency was turned into a new state variable, integrating the phase update:

$$\dot{\omega}(t) = \nu F(t) \cos \phi(t). \quad (2)$$

From (2), it can be established that the integrator argument sums up to zero over one period (i.e. ω converges) if the frequency ω is equal to the frequency of the input signal.

The adaptive oscillator input $F(t)$ was the difference between the elbow angular position $\theta(t)$ (measured by the device encoder) and the learned (i.e. estimated) position of the elbow $\hat{\theta}(t)$: $F(t) = \theta(t) - \hat{\theta}(t)$, this estimated position being the oscillator output plus the offset $\alpha_0(t)$:

$$\hat{\theta}(t) = \alpha_0 + \alpha_1 \sin \phi(t). \quad (3)$$

The offset $\alpha_0(t)$ and the amplitude $\alpha_1(t)$ were finally learned by the following two integrators:

$$\dot{\alpha}_0(t) = \eta F(t) \quad \dot{\alpha}_1(t) = \eta F(t) \sin \phi(t), \quad (4)$$

where η is the integrator gain.

Assuming the elbow movement to be (quasi-)sinusoidal, the same adaptive oscillator can further provide an estimate of the elbow velocity and acceleration:

$$\hat{\theta}(t) = \alpha_1 \omega(t) \cos \phi(t) \quad (5)$$

$$\hat{\dot{\theta}}(t) = -\alpha_1(t) \omega(t)^2 \sin \phi(t). \quad (6)$$

As in [13], we used the values $\nu = 20$ and $\eta = 5$ for the learning parameter and the integrator gain, respectively. Good behavior using these parameters was confirmed during pilot tests.

B. Elbow assistance

We assumed that the dynamics of the elbow were governed by a pendulum-like differential equation for the angular position $\theta(t)$:

$$I\ddot{\theta}(t) + b\dot{\theta}(t) + mgl \sin \theta(t) \approx I\ddot{\theta}(t) + b\dot{\theta}(t) + mgl\theta(t) = \tau_{tot}(t), \quad (7)$$

where I , b , m , and l denote the inertia, damping coefficient, total mass, and equivalent length of the elbow+forearm, and g denotes the constant of gravity. The approximation relies on the small angle assumption, i.e. $\sin \theta \approx \theta$. The total torque $\tau_{tot}(t)$ was composed by the torque provided by the human $\tau_h(t)$ plus the torque provided by the assistive device $\tau_d(t)$: $\tau_{tot}(t) = \tau_h(t) + \tau_d(t)$. The device was assumed to be transparent to the user, such that its inertia, friction, and mass were not taken into account in (7).

The control algorithm was based on an estimation of the total torque $\hat{\tau}_{tot}(t)$ by plugging Equations (3), (5), and (6) into (7), to obtain an inverse model:

$$\hat{\tau}_{tot}(t) = \hat{I}\hat{\ddot{\theta}}(t) + \hat{b}\hat{\dot{\theta}}(t) + \hat{m}g\hat{l}\hat{\theta}(t), \quad (8)$$

where \hat{I} , \hat{b} , \hat{m} , and \hat{l} are estimates of the corresponding actual variables. Finally, the device provided a fraction of this estimated torque to the human in order to assist the movement:

$$\tau_d(t) = \kappa \hat{\tau}_{tot}(t), \quad (9)$$

where κ is the level of assistance. In theory, $\kappa = 1$ is the upper limit, corresponding to the situation where the participant should perform the movement without providing any torque. However, preliminary tests revealed that it was not possible to provide assistance larger than $\kappa = 1/3$ with our device, due to torque saturations, model approximations, and stability issues. With this setting, the device should provide about one third of the total torque.

Plugging (9) into (7), and assuming that the estimated kinematic variables ($\hat{\theta}$, $\hat{\dot{\theta}}$, $\hat{\ddot{\theta}}$) were equal to the actual ones, we obtain a resulting dynamical system, which corresponds to what a human should perceive when assisted:

$$\tilde{I}\ddot{\theta}(t) + \tilde{b}\dot{\theta}(t) + \tilde{m}g\tilde{l}\theta(t) = \tau_h(t), \quad (10)$$

where $\tilde{I} = I - \kappa\hat{I}$, $\tilde{b} = b - \kappa\hat{b}$, and $\tilde{m}\tilde{l} = ml - \kappa\hat{m}\hat{l}$ are the resulting perceived parameters.

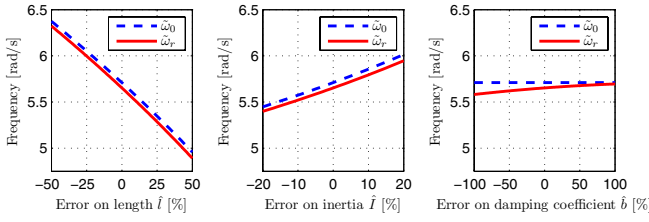


Fig. 1. Variation of the predicted frequencies $\tilde{\omega}_0$ (dashed blue) and $\tilde{\omega}_r$ (solid red) as a function of errors [%] on the estimated equivalent length \tilde{l} , inertia \tilde{I} and damping coefficient \tilde{b} .

C. Error in parameter identification: Model-based predictions

The system's resonance frequency can be calculated from (10):

$$\omega_r = \omega_0 \sqrt{1 - 2\zeta^2}, \quad (11)$$

where

$$\omega_0 = \sqrt{\frac{\tilde{m}g\tilde{l}}{\tilde{I}}} \quad (12)$$

is the natural frequency, i.e. the resonance frequency of the undamped dynamics, and $\zeta = \tilde{b}/(2\tilde{I}\omega_0)$ is the damping factor.

As shown in Equations (11) and (12), the natural and resonance frequencies vary as a function of the system's parameters \tilde{I} , \tilde{b} , \tilde{m} , and \tilde{l} . However, if the system's parameters are correctly estimated (i.e. if $\tilde{I} = I$, etc. . .), the natural and resonance frequencies should not change with the level of assistance κ .

Let us now assume that the system's parameters are not correctly estimated, i.e.:

$$\hat{I} = (1 + e_I) I \quad \hat{b} = (1 + e_b) b \quad \hat{l} = (1 + e_l) l, \quad (13)$$

where e_I , e_b , and e_l denote the errors of the corresponding variables. Error in the estimate of the mass would have the same effect as error on the equivalent length, and is therefore not investigated.

Model predictions for the variation of the natural and resonance frequencies as a function of the wrongly estimated parameters are shown in Figure 1, using the forearm intrinsic parameters of a representative participant.

Assuming that the participant performed the movement at the resonance frequency, which was therefore adapted as a function of the resulting dynamics, the results shown in Figure 1 lead to the following predictions:

- overestimating the equivalent length \hat{l} should lead to a smaller movement frequency, and vice-versa;
- overestimating the inertia \hat{I} should lead to a larger movement frequency, and vice-versa;
- overestimating the damping coefficient \hat{b} should lead to a larger movement frequency, and vice-versa.

In addition, we point out that the influence of the errors on the estimation of \hat{I} and \hat{l} is higher than the influence of the error on the damping coefficient \hat{b} . This will be investigated by sensitivity analyses.

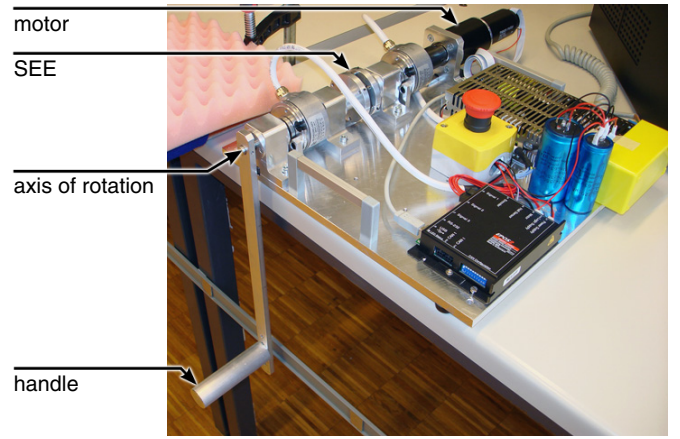


Fig. 2. Top view of the assistive device.

D. Participants

Five healthy, male participants took part to the experiment (age: 20-30years, weight: 60-90kg). The forearm mass m , equivalent length l , and inertia I were individually estimated for each participant, using standard tables from [22]:

$$\begin{aligned} m &= 0.022M_{body} \text{ [kg]} \\ l &= 0.682L_{forearm} \text{ [m]} \\ I &= m(0.827L_{forearm})^2 \text{ [Nms}^2/\text{rad]} \end{aligned}$$

where M_{body} and $L_{forearm}$ denote the total body weight and the total forearm length, respectively. For all participants, we used the damping ratio $\zeta = 0.1$, i.e. approximately half smaller than documented in the literature for similar movements around the upward vertical position [23]. This was obtained after manual tuning during preliminary tests.

E. Experimental setup

The assistive device used for the experiments was a simple one DOF pendulum, parallel to the participant's forearm, and controlled by a motor through a series elastic element (SEE). Figure 2 shows a top view of the assistive device. The SEE introduces compliance and achieves series elastic actuation [8], [24], [25], such that the assistive torque can be perfectly controlled within the bandwidth of interest: $\tau_d = k_{SEE}\Delta\theta$, where k_{SEE} is the SEE stiffness, which is known, and $\Delta\theta$ is the SEE deformation, which is measured by two encoders, one at each side of the SEE (see later). The assistive torque τ_d is controlled by setting $\Delta\theta$ to the desired value.

Since the participant's forearm was not constrained, the rotation axis of the elbow can be continuously aligned with the one of the assistive device. As consequence, there is no need for additional passive degrees of freedom for axes alignment.

The SEE was made of two disks: one coupled to the motor and the other to the pendulum, and both connected to each other via six tangential traction springs. The resulting torque provided by the SEE was close to a linear function of the deviation angle between the disks. The SEE stiffness was estimated to $k_{SEE} = 3.8\text{Nm/rad}$. The deviation angle between

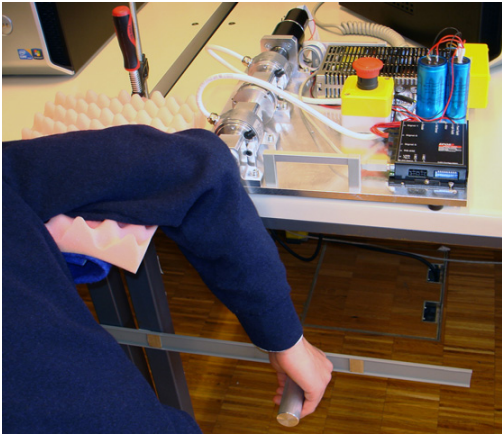


Fig. 3. Side view of a participant using the assistive device.

the two disks was mechanically limited to $0.3rad$, resulting in a maximal supplied torque of about $\tau_{d,max} = 1.14Nm$.

The motor actuating the device was a Maxon DC Motor RE 40 #148877 (Maxon Motors, Sachseln, Switzerland). The motor low level control (i.e. PID controllers for current and position control), as well as current limitations to keep the motor torque within safe boundaries (current limited to 2.63A, such that output torque was limited to 15Nm after the gearbox) were directly handled by the supplied motor controller, i.e. a Maxon EPOS2 50/5.

The high level control, i.e. the adaptive oscillator and the assistive protocol, was implemented using MATLAB and Simulink (the Mathworks, Natick, MA). To get the algorithm running close to real-time, we implemented a ‘‘Soft Real Time’’ block in Simulink which guaranteed a more or less constant sampling rate of 15ms.

The position of the motor and the elbow were measured with two incremental encoders RI 58-D (Hengstler, Aldingen, Germany) with 5000 pulses resulting in a resolution of 0.018° .

F. Experimental protocol

Participants sat on a chair while having the right upper arm resting horizontally on a support mounted on a table and the forearm hanging down, as shown in Figure 3. They were asked to grab a handle attached to the assistive device, and to make cyclical flexion/extension of the elbow about the vertical downward position.

Participants wore a hearing protector to decrease potential auditory feedback from the motor noise, and had direct visual feedback about the forearm movement. The instruction was to oscillate at a constant amplitude specified by two visual markers. Importantly, the movement frequency was left free and the participants were asked to oscillate at the most comfortable frequency.

Before doing the actual data acquisition, a training sequence of seven minutes was given to the participants, in order to become familiar with the device. This sequence was made of seven trials of one minute each, alternating between no assistance ($\kappa = 0$), and movement assistance of $\kappa = 1/3$.

After this training sequence, all participants reported to be relaxed with the device and the assistance. Moreover, visual inspection of the data revealed that they had all found a steady-state movement frequency. Data corresponding to the training sequence were not used for the analyses.

After a short break, participants did a second sequence lasting fifteen minutes. Again, this sequence was made up with a series of fifteen one-minute-long trials, alternating between no assistance ($\kappa = 0$), and assistance with $\kappa = 1/3$. On top of that, during the seven trials with assistance, an error in the estimation of the equivalent length e_l , inertia e_I , or damping coefficient e_b of the human forearm model was introduced. The different conditions were individually randomized for each participant, and comprised the following:

- ($e_l = -50\%$, $e_I = 0$, $e_b = 0$), denoted \hat{l}_- ,
- ($e_l = +50\%$, $e_I = 0$, $e_b = 0$), denoted \hat{l}_+ ,
- ($e_l = 0$, $e_I = -20\%$, $e_b = 0$), denoted \hat{I}_- ,
- ($e_l = 0$, $e_I = +20\%$, $e_b = 0$), denoted \hat{I}_+ ,
- ($e_l = 0$, $e_I = 0$, $e_b = -100\%$), denoted \hat{b}_- ,
- ($e_l = 0$, $e_I = 0$, $e_b = +100\%$), denoted \hat{b}_+ ,
- and ($e_l = 0$, $e_I = 0$, $e_b = 0$), i.e. no error, denoted $\hat{l}/\hat{I}/\hat{b}_0$.

G. Data processing and statistical analyses

The measured position of the elbow $\theta(t)$ was low pass filtered using a forward/backward Butterworth filter of 3rd order with a cutoff frequency of 4Hz. Moreover, the movement offset was filtered out by passing the signal through a similar lowpass Butterworth filter, but with a cutoff frequency of 0.1Hz, and by subtracting this signal to the original one.

Movement frequency was estimated by extracting the zero crossings of the filtered signal to calculate its instantaneous period. The instantaneous frequency was calculated by taking the inverse of the period and multiplying by 2π .

To compare the measured frequencies between the different conditions, statistics were performed on the data from the second half of each trial, such that only steady-state performance was analyzed. To establish the significance of the different observed movement frequencies, we performed Wilcoxon rank-sum tests. This test reveals whether the median of two different populations are different.

To establish whether the observed movement frequencies complied with quantitative predictions from the model, we performed sensitivity analyses, i.e. we calculated the sensitivity of the steady-state frequency with respect to the three parameters. For the equivalent length, this was equal to:

$$S_l^\omega = \frac{\Delta\bar{\omega}_l}{\bar{\omega}_{l_0}} \cdot \frac{\hat{l}_0}{\Delta\hat{l}}, \quad (14)$$

where $\Delta\bar{\omega}_l = \bar{\omega}_{l_+} - \bar{\omega}_{l_-}$; $\bar{\omega}_{l_-}$, $\bar{\omega}_{l_0}$, $\bar{\omega}_{l_+}$ denote the medians of the measured frequency during the corresponding conditions; and $\Delta\hat{l}/\hat{l}_0 = 100\%$, since errors of $\pm 50\%$ were tested. Similar sensitivities were computed for the inertia and the damping coefficient, S_I^ω and S_b^ω , respectively, with $\Delta\hat{I}/\hat{I}_0 = 40\%$ and $\Delta\hat{b}/\hat{b}_0 = 200\%$.

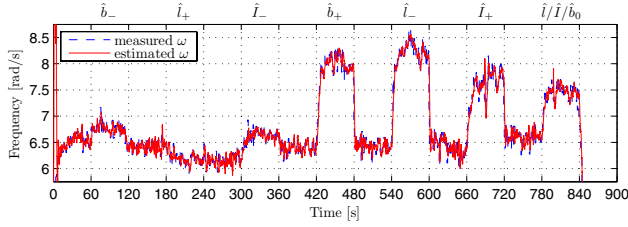


Fig. 4. Evolution of the measured frequency (dashed blue) and the estimated frequency by the adaptive oscillator (solid red) in time. The label on top of the graph shows the condition for the corresponding trial.

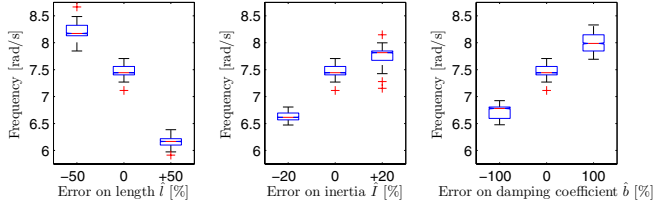


Fig. 5. Movement frequency for the different conditions, i.e. as a function of the error on the estimated equivalent length \hat{l} , inertia \hat{I} , and damping coefficient \hat{b} .

III. RESULTS

A. Movement frequency

Figure 4 shows both the “actual” instantaneous frequency (computed from the measured position) and the estimated frequency ω from the adaptive oscillator during the whole sequence of a representative participant. Both fit very well, as shown in the figure.

Figure 5 shows the steady-state frequencies of a representative participant in the different conditions. Variations are clearly visible across conditions, and, as expected from model predictions, a positive error on the length e_l induced smaller frequency, and a positive error on the inertia e_I or on the friction coefficient e_b induced larger movement frequency. Note that the frequency ranges are slightly different between the model predictions and the experiments, since the predictions were made with the dynamical arm properties of a single of the five participants. Moreover, we did not take the dynamical properties of the device into account in this model, for the sake of simplicity. Again, what is really important here, is the good matching between the relative changes across the different cases.

Table I shows the results for all participants, such that 9 (tests/participant) \times 5 (participants) = 45 tests were performed. Wilcoxon rank-sum tests revealed that these 45 comparisons all reached significance on the population medians, with a confidence level of more than 99.9%. Regarding the predictions, 39 (87%) of these tests validated the model-based assumptions (as shown by a \checkmark in Table I) and 6 (13%) revealed a trend being opposed to the corresponding model-based assumption (as shown by a \times in Table I).

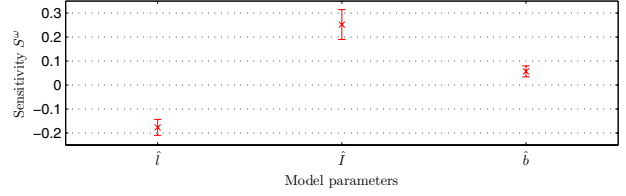


Fig. 6. Sensitivity of the movement frequency to variations in the estimated model parameters, namely the equivalent length \hat{l} , inertia \hat{I} , and damping coefficient \hat{b} . Mean \pm standard error of the mean among the 5 participants.

B. Sensitivity analysis

The model predicted that the changes in resonance frequency have not the same sensitivity to changes in the different estimated parameters. For instance, an overestimation of \hat{I} and \hat{b} should both lead to larger resonance frequency (as observed for most of the participants, see Table I), but at a much higher rate (higher slope) for \hat{I} than \hat{b} . This can be observed from the slopes in Figure 1.

To establish whether the observed movement frequencies complied with these quantitative predictions, we performed sensitivity analyses, as explained in Section II-G. The results are shown in Figure 6, and are coherent with the model-based predictions. As expected, S_l^ω and S_I^ω are higher in absolute value than S_b^ω , and the sensitivity to the error in equivalent length S_l^ω is negative, while the other two are positive.

The small sensitivity of the participants behavior to the estimate of the damping coefficient is a good point to establish the robustness of our assistive method to model approximations, since the damping coefficient b is by far the most difficult parameter to estimate.

IV. CONCLUSION

In this paper, we presented a simple device to test new control approaches for assistance and rehabilitation, by supporting the elbow during rhythmic flexion-extension movements. Our approach was based on an adaptive oscillator learning the high-level features of the movement while remaining synchronized in phase and frequency. The results showed that the frequency estimated by the adaptive oscillator fitted very well the actual frequency of the movement. Furthermore, we demonstrated that the adaptation of the participant’s movement frequency generally corresponded to theoretical predictions, when large errors were purposely introduced in the inverse model parameters. From a sensitivity analysis, we demonstrated the high robustness of our method to model approximations, because:

- the sensitivity of all tested parameters was generally low (< 0.3 in absolute value);
- the parameters having the highest absolute sensitivity (mass, equivalent length, and inertia) were the easiest to estimate [26];
- the friction coefficient, which was by far more difficult to properly estimate and was likely different to the simple proposed linear model, only marginally influenced the resulting movement frequency.

TABLE I

ACCORDANCE OF THE RELATIONSHIPS BETWEEN MEDIANS OF MEASURED FREQUENCY FOR TWO DIFFERENT CONDITIONS WITH THE MODEL-BASED PREDICTIONS. ALL p -VALUES ARE STATISTICALLY SIGNIFICANT ($p < 0.001$).

	$\omega_{i_-} > \omega_{i_0}$	$\omega_{i_0} > \omega_{i_+}$	$\omega_{i_-} > \omega_{i_+}$	$\omega_{j_-} < \omega_{i_0}$	$\omega_{i_0} < \omega_{i_+}$	$\omega_{j_-} < \omega_{i_+}$	$\omega_{b_-} < \omega_{b_0}$	$\omega_{b_0} < \omega_{b_+}$	$\omega_{b_-} < \omega_{b_+}$
Participant 1	✓ $p < 0.001$								
Participant 2	✓ $p < 0.001$	✓ $p < 0.001$	✓ $p < 0.001$	✗ $p < 0.001$	✓ $p < 0.001$				
Participant 3	✓ $p < 0.001$	✓ $p < 0.001$	✓ $p < 0.001$	✓ $p < 0.001$	✗ $p < 0.001$	✓ $p < 0.001$	✗ $p < 0.001$	✓ $p < 0.001$	✓ $p < 0.001$
Participant 4	✓ $p < 0.001$	✗ $p < 0.001$	✗ $p < 0.001$	✗ $p < 0.001$					
Participant 5	✓ $p < 0.001$								

In conclusion, this paper showed that oscillator-based protocols are very relevant for assistive/rehabilitation robotics, due to a high robustness in the model parameters. This permits to design protocols that keep constant the overall movement frequency with or without assistance. This finding complements the other advantages of the approach that were already pointed out in [13]: simple and cheap sensing, adaptivity (targeting “assist-as-needed” protocols), and intuitive interaction for the participants.

ACKNOWLEDGMENT

This work was supported by the EU within the EVRYON Collaborative Project STREP (FP7-ICT-2007-3-231451).

REFERENCES

- [1] S. Schaal, “The new robotics — towards human-centered machines,” *HFSP Journal*, vol. 1, no. 2, pp. 115–26, 2007.
- [2] A. Dollar and H. Herr, “Lower extremity exoskeletons and active orthoses: Challenges and state-of-the-art,” *Robotics, IEEE Transactions on*, vol. 24, no. 1, pp. 144–158, Feb. 2008.
- [3] D. P. Ferris, “The exoskeletons are here,” *J Neuroeng Rehabil*, vol. 6, p. 17, 2009.
- [4] B. Dellon and Y. Matsuoka, “Prosthetics, exoskeletons, and rehabilitation [grand challenges of robotics],” *Robotics Automation Magazine, IEEE*, vol. 14, no. 1, pp. 30–34, march 2007.
- [5] G. Colombo, M. Wirz, and V. Dietz, “Driven gait orthosis for improvement of locomotor training in paraplegic patients,” *Spinal Cord*, vol. 39, no. 5, pp. 252–255, May 2001.
- [6] K. P. Westlake and C. Patten, “Pilot study of lokomat versus manual-assisted treadmill training for locomotor recovery post-stroke,” *J Neuroeng Rehabil*, vol. 6, p. 18, 2009.
- [7] E. T. Wolbrecht, V. Chan, D. J. Reinkensmeyer, and J. E. Bobrow, “Optimizing compliant, model-based robotic assistance to promote neurorehabilitation,” *IEEE Trans Neural Syst Rehabil Eng*, vol. 16, no. 3, pp. 286–297, Jun 2008.
- [8] H. Vallery, J. Veneman, E. van Asseldonk, R. Ekkelenkamp, M. Buss, and H. van Der Kooij, “Compliant actuation of rehabilitation robots,” *IEEE Robotics Automation Magazine*, vol. 15, no. 3, pp. 60–69, Sep. 2008.
- [9] R. Riener, L. Lünenburger, S. Jezernik, M. Anderschitz, G. Colombo, and V. Dietz, “Patient-cooperative strategies for robot-aided treadmill training: first experimental results,” *IEEE Trans Neural Syst Rehabil Eng*, vol. 13, no. 3, pp. 380–394, Sep 2005.
- [10] J. Rosen, M. Brand, M. B. Fuchs, and M. Arcan, “A myosignal-based powered exoskeleton system,” *IEEE Transactions on Systems, Man and Cybernetics, Part A*, vol. 31, no. 3, pp. 210–222, May 2001.
- [11] K. Kiguchi, K. Iwami, M. Yasuda, K. Watanabe, and T. Fukuda, “An exoskeletal robot for human shoulder joint motion assist,” *Mechatronics, IEEE/ASME Transactions on*, vol. 8, no. 1, pp. 125–135, march 2003.
- [12] R. Ronsse, N. Vitiello, T. Lenzi, J. van den Kieboom, M. Chiara Carrozza, and A. J. Ijspeert, “Adaptive oscillators with human-in-the-loop: Proof of concept for assistance and rehabilitation,” in *Biomedical Robotics and Biomechanics (BioRob), 2010 3rd IEEE RAS and EMBS International Conference on*, Sep. 2010, pp. 668–674.
- [13] R. Ronsse, N. Vitiello, T. Lenzi, J. van den Kieboom, M. C. Carrozza, and A. J. Ijspeert, “Human-robot synchrony: flexible assistance using adaptive oscillators,” *IEEE Trans Biomed Eng*, vol. in press, 2010.
- [14] L. Righetti, J. Buchli, and A. J. Ijspeert, “Dynamic hebbian learning in adaptive frequency oscillators,” *Physica D*, vol. 216, pp. 269–281, 2006.
- [15] J. Buchli, L. Righetti, and A. J. Ijspeert, “Frequency analysis with coupled nonlinear oscillators,” *Physica D*, vol. 237, pp. 1705–1718, 2008.
- [16] T. Lenzi, S. De Rossi, N. Vitiello, A. Chiri, S. Roccella, F. Giovacchini, F. Vecchi, and M. C. Carrozza, “The neuro-robotics paradigm: NEURARM, NEUROExos, HANDEXOS,” in *Proc. Annual International Conference of the IEEE Engineering in Medicine and Biology Society EMBC 2009*, Sep. 3–6, 2009, pp. 2430–2433.
- [17] B. W. Verdaasdonk, H. F. J. M. Koopman, and F. C. T. Van Der Helm, “Resonance tuning in a neuro-musculo-skeletal model of the forearm,” *Biol Cybern*, vol. 96, no. 2, pp. 165–180, Feb 2007.
- [18] M. L. Latash, “Virtual trajectories, joint stiffness, and changes in the limb natural frequency during single-joint oscillatory movements,” *Neuroscience*, vol. 49, no. 1, pp. 209–220, Jul 1992.
- [19] M. O. Abe and N. Yamada, “Modulation of elbow joint stiffness in a vertical plane during cyclic movement at lower or higher frequencies than natural frequency,” *Exp Brain Res*, vol. 153, no. 3, pp. 394–399, Dec 2003.
- [20] O. White, Y. Bleyenheuft, R. Ronsse, A. M. Smith, J.-L. Thonnard, and P. Lefèvre, “Altered gravity highlights central pattern generator mechanisms,” *J Neurophysiol*, vol. 100, no. 5, pp. 2819–2824, Nov 2008.
- [21] L. Righetti, J. Buchli, and A. J. Ijspeert, “Adaptive frequency oscillators and applications,” *The Open Cybernetics and Systemics Journal*, vol. 3, pp. 64–69, 2009.
- [22] D. A. Winter, *Biomechanics and Motor Control of Human Movement*, 4th ed. New Jersey: Wiley, 2009.
- [23] C.-C. Lin, M.-S. Ju, and C.-W. Lin, “The pendulum test for evaluationg spasticity of the elbow joint,” *Arch Phys Med Rehabil*, vol. 84, no. 1, pp. 69–74, Jan. 2003.
- [24] G. A. Pratt and M. M. Williamson, “Series elastic actuators,” in *Proc. IEEE/RSJ International Conference on Intelligent Robots and Systems 95. Human Robot Interaction and Cooperative Robots*, vol. 1, Aug. 5–9, 1995, pp. 399–406.
- [25] M. Zinn, B. Roth, O. Khatib, and J. K. Salisbury, “A new actuation approach for human friendly robot design,” *The International Journal of Robotics Research*, vol. 23, no. 4-5, pp. 379–398, 2004.
- [26] V. Zatsiorsky, V. Seluyanov, and L. Chugunova, “Methods of determining mass-inertial characteristics of human body segments,” in *Contemporary problems of biomechanics*, G. Chernyi and S. Regirer, Eds. Moscow/Boca Raton: Mir Publishers/CRC Press, 1990, pp. 272–291.